

How is the Reactivity of Cytochrome P450cam Affected by Thr252X Mutation? A QM/MM Study for X = Serine, Valine, Alanine, Glycine

Muhannad Altarsha, Tobias Benighaus, Devesh Kumar, and Walter Thiel*

Max-Planck-Institut für Kohlenforschung, Kaiser-Wilhelm-Platz 1,
D-45470 Mülheim an der Ruhr, Germany

Received November 7, 2008; E-mail: thiel@mpi-muelheim.mpg.de

Abstract: Proton transfer reactions play a vital role in the catalytic cycle of cytochrome P450cam and are responsible for the formation of the iron-oxo species called Compound I (Cpd I) that is supposed to be the active oxidant. Depending on the course of the proton transfer, protonation of the last observable intermediate (ferric hydroperoxo complex, Cpd 0) can lead to either the formation of Cpd I (coupling reaction) or the ferric resting state (uncoupling reaction). The ratio of these two processes is drastically affected by mutation of the Thr252 residue. In this work, we study the effect of Thr252X (X = serine, valine, alanine, glycine) mutations on the formation of Cpd I by means of hybrid quantum mechanical/molecular mechanical (QM/MM) calculations and classical simulations. In the wild-type enzyme, the coupling reaction is favored since its rate-limiting barrier is 13 kcal/mol lower than that for uncoupling. This difference is reduced to 7 kcal/mol in the serine mutant. In the case of valine, alanine, and glycine mutants, an additional water molecule enters the active site and lowers the activation energy of the uncoupling reaction significantly. With the additional water molecule, coupling and uncoupling have similar barriers in the valine mutant, and the uncoupling reaction becomes favored in the alanine and glycine mutants. These findings agree very well with experimental results and thus confirm the assumption that uncontrolled proton delivery by solvent water networks is responsible for the uncoupling reaction. The present study provides a detailed mechanistic understanding of the role of the Thr252 residue.

I. Introduction

The heme protein monooxygenases known as cytochrome P450 play a vital role in the metabolism of xenobiotic substances in plants, fungi, bacteria, insects, and mammals.^{1–3} They catalyze a variety of reactions including hydroxylation, epoxidation, and heteroatom oxidation. The consensus mechanism of P450 hydroxylation is shown in Scheme 1, where the proximal cysteinate ligand is abbreviated as L, and the porphyrin macrocycle is symbolized by the two bold lines flanking the iron.⁴ The catalytic cycle begins with the resting state (S1) in which a water molecule is bound to the ferric ion in the distal side. When a substrate enters the protein pocket, the water molecule is displaced from the reactive center, leaving a ferric substrate-bound state (ferric resting state, S2). This complex is a slightly better electron acceptor than the resting state and can therefore take up an electron from reductase protein, leading to a high-spin ferrous complex (S3). Subsequent binding of molecular oxygen produces the oxyferrous state (S4). Addition of a second electron yields a peroxo-ferric derivative (S5) that, upon protonation of the distal oxygen, forms a hydroperoxo-

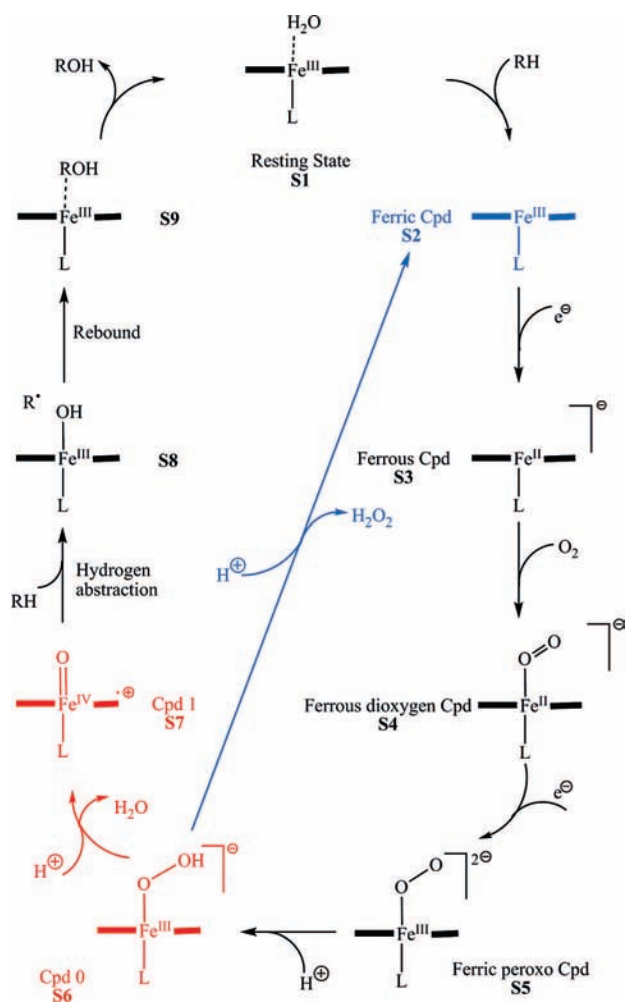
ferric intermediate which is also known as Compound 0 (Cpd 0, S6). A second protonation then leads to O–O bond cleavage with loss of a water molecule and generates the “active oxygen” in the putatively active oxoferryl species Compound I (Cpd I, S7). Alternatively, protonation of the proximal oxygen of Cpd 0 (S6) leads to release of hydrogen peroxide and regenerates the ferric resting state (S2 in Scheme 1).

In recent years, much attention has focused on possible mechanisms for the required proton delivery to the active site. On the basis of extensive site-directed mutation studies,^{5–10} it has been suggested that the Asp251 and Thr252 residues participate in a controlled proton delivery pathway that involves solvent water and provides an active-site H-bond donor, which may be a trapped water molecule rather than Thr252.^{5,8} The Thr252 residue is highly conserved in P450cam crystal structures and is believed to play an important role in the dioxygen activation machinery.¹¹

- (1) Guengerich, F. P. *J. Biol. Chem.* **1991**, *266*, 10019–10022.
- (2) Porter, T. D.; Coon, M. J. *J. Biol. Chem.* **1991**, *266*, 13469–13472.
- (3) (a) Ortiz de Montellano, P. R. *Cytochrome P450: Structure, Mechanism and Biochemistry*, 2nd ed.; Plenum Press: New York, 1995. (b) Ortiz de Montellano, P. R. *Cytochrome P450: Structure, Mechanism and Biochemistry*, 3rd ed.; Plenum Press: New York, 2005.
- (4) Davydov, R.; Macdonald, I. D. G.; Makris, T. M.; Sugar, S. G.; Hoffman, B. M. *J. Am. Chem. Soc.* **1999**, *121*, 10654–10655.

- (5) Vidakovic, M.; Sligar, S. G.; Li, H.; Poulos, T. L. *Biochemistry* **1998**, *37*, 9211–9219.
- (6) Martinis, S. A.; Atkins, W. M.; Stayton, P. S.; Sligar, S. G. *J. Am. Chem. Soc.* **1989**, *111*, 9252–9253.
- (7) Imai, M.; Shimada, H.; Watanabe, Y.; Matsuhima-Hibiya, Y.; Makino, R.; Koga, H.; Horiuchi, T.; Ishimura, Y. *Proc. Natl. Acad. Sci. U.S.A.* **1989**, *86*, 7823–7827.
- (8) Gerber, N. C.; Sligar, S. G. *J. Biol. Chem.* **1994**, *269*, 4260–4266.
- (9) Gerber, N. C.; Sligar, S. G. *J. Am. Chem. Soc.* **1992**, *114*, 8742–8743.
- (10) Benson, D. E.; Suslick, K. S.; Sligar, S. G. *Biochemistry* **1997**, *36*, 5104–5107.

Scheme 1. Cytochrome P450cam Reaction Cycle



Site-directed mutagenesis studies^{6–9} indicate that the presence of Thr252 is essential for the formation of Cpd I in P450cam. Upon replacement by an aliphatic residue in mutants such as Thr252Ala (T252A)^{7,12} and Thr252Gly (T252G),⁷ there is an uncoupling of O₂ consumption from camphor hydroxylation: most of O₂ consumed is converted to H₂O₂ without O–O bond cleavage,⁷ and only 5% (3%) of the T252A (T252G) mutants undergo hydroxylation. By contrast, in the wild-type enzyme, the coupling ratio of O₂ consumption and hydroxylation is 100%. According to a low-temperature EPR and ENDOR study, both wild-type P450cam and the T252A mutant form Cpd 0 at 77 K, but only the former gives hydroxylation upon warming while the latter shows uncoupling, thus confirming the key role of Thr252 during the delivery of the second proton in the catalytic cycle (from S6 to S7).⁴ Given that Cpd I formation is suppressed in the T252A mutant, the observed reactivity toward other substrates may suggest the existence of more than one oxidant in P450 enzymes.¹³ For example, the T252A mutant is capable of epoxidizing the double bond of olefins such as 5-methyl-encamphor, presumably with Cpd 0 being the active species

in this case.¹⁴ However, Cpd 0 is generally found to be a sluggish oxidant that is not competitive with Cpd I and may only function as such in the absence of Cpd I.^{14–17}

Substitution of Thr252 with valine (T252V) also causes a considerable uncoupling of oxygen consumption and hydroxylation, with about 30–40% of hydrogen peroxide formation.^{7,18} Substitution with serine (T252S), a hydroxyamino acid, has a smaller effect: only approximately 15% of O₂ consumed is recovered as H₂O₂.^{7,18,19} Replacing the Thr252 side-chain hydroxyl (OH) with a methoxy (OCH₃) group slows the hydroxylation reaction significantly, but the yield of 5-exohydroxycamphor is still 100% (no uncoupling).¹⁹

Taken together, these experimental findings indicate that the Thr252 residue plays a crucial mechanistic role and influences the ratio of hydroxylation versus uncoupling products. Although a free hydroxy group at position 252 is not a prerequisite for O–O bond cleavage in P450cam, the replacement of Thr252 by amino acids with non-hydrogen-bonding side chains virtually suppresses camphor hydroxylation in favor of the uncoupled reduction of O₂ to H₂O₂.^{7,18,20}

In the crystal structure of the T252A mutant, there is a water molecule near the O₂ binding site of the mutant which is not present in the wild-type enzyme.^{11,21} This suggests that the solvent may be responsible for the observed uncoupling of the enzyme turnover from camphor hydroxylation in the mutant.^{12,21} Solvent in contact with dioxygen may supply protons in an uncontrolled manner, promoting H₂O₂ production, rather than substrate hydroxylation.

The available crystal structures²² of wild-type P450cam indicate three possible proton delivery pathways through the Asp251,^{5,23,24} Glu366,^{22,25} and Arg299²⁶ channels. The latter has been characterized through a combined site-directed mutagenesis and molecular dynamics study²⁷ but is blocked when substrate is present. In the Glu366 channel, the bridging water molecules (nos. 687, 566, 523, and 902 in PDB structure 1DZ8²²) and the hydroxyl group of Thr252 form a network connecting the carboxyl group of Glu366 and the distal oxygen atom, which however terminates at Glu366 without any connection to the surface.⁵ In this paper, we shall therefore focus on the Asp251 channel only.

- (11) Raag, R.; Martinis, S. A.; Sligar, S. G.; Poulos, T. L. *Biochemistry* **1991**, *30*, 11420–11429.
 (12) Nagano, S.; Cupp-Vickery, J. R.; Poulos, T. L. *J. Biol. Chem.* **2005**, *280*, 22102–22107.
 (13) Denisov, I. G.; Makris, T. M.; Sligar, S. G.; Schlichting, I. *Chem. Rev.* **2005**, *105*, 2253–2278.

- (14) Jin, S.; Makris, T. M.; Bryson, T. A.; Sligar, S. G.; Dawson, J. H. *J. Am. Chem. Soc.* **2003**, *125*, 3406–3407.
 (15) De Visser, S. P.; Kumar, D.; Shaik, S. J. *Inorg. Biochem.* **2004**, *98*, 1183–1193.
 (16) Li, C.; Zhang, L.; Zhang, C.; Hirao, H.; Wu, W.; Shaik, S. *Angew. Chem., Int. Ed.* **2007**, *46*, 8168–8170.
 (17) Hirao, H.; Kumar, D.; Shaik, S. J. *Inorg. Biochem.* **2006**, *100*, 2054–2068.
 (18) Shimada, H.; Makino, R.; Imai, M.; Horiuchi, T.; Ishimura, Y. Mechanism of Oxygen Activation by Cytochrome P-450cam. *International Symposium on Oxygenases and Oxygen Activation*; Yamada Science Foundation, 1990; pp 133–136.
 (19) Kimata, Y.; Shimada, H.; Hirose, T.; Ishimura, Y. *Biochem. Biophys. Res. Commun.* **1995**, *208*, 96–102.
 (20) Aikens, J.; Sligar, S. G. *J. Am. Chem. Soc.* **1994**, *116*, 1143–1144.
 (21) Hishiki, T.; Shimada, H.; Nagano, S.; Egawa, T.; Kanamori, Y.; Makino, R.; Park, S. Y.; Adachi, S. I.; Shiro, Y.; Ishimura, Y. *J. Biochem.* **2000**, *128*, 965–974.
 (22) Schlichting, I.; Berendzen, J.; Chu, K.; Stock, A. M.; Maves, S. A.; Benson, D. E.; Sweet, R. M.; Ringe, D.; Petsko, G. A.; Sligar, S. G. *Science* **2000**, *287*, 1615–1622.
 (23) Taraphder, S.; Hummer, G. *J. Am. Chem. Soc.* **2003**, *125*, 3931–3940.
 (24) Kamachi, T.; Yoshizawa, K. *J. Am. Chem. Soc.* **2003**, *125*, 4652–4661.
 (25) Guallar, V.; Friesner, R. A. *J. Am. Chem. Soc.* **2004**, *126*, 8501–8508.
 (26) Oprea, T. I.; Hummer, G.; Garcia, A. E. *Proc. Natl. Acad. Sci. U.S.A.* **1997**, *94*, 2133–2138.
 (27) Loida, P. J.; Sligar, S. G.; Paulsen, M. D.; Arnold, G. E.; Ornstein, R. L. *J. Biol. Chem.* **1995**, *270*, 5326–5330.

Previous theoretical studies have addressed the formation of Cpd I from Cpd 0 in the wild-type enzyme using gas-phase model systems.^{23,25,28–32} In the most elaborate such work, density functional theory (DFT) calculations on a large active site model with 96 atoms predict the existence of a protonated Cpd 0 species with significant barriers for the conversion both toward Cpd 0 and Cpd I.³⁰ According to a later quantum mechanics/molecular mechanics (QM/MM) study,³³ protonation of Cpd 0 by Glu366 via a hydrogen-bonding network may indeed generate such an intermediate, which however is very high in energy (more than 20 kcal/mol above Cpd 0) and mechanistically irrelevant since the barrier for its decay is only 3–4 kcal/mol both toward Cpd 0 and Cpd I. The QM/MM calculations suggest another mechanism instead: an initial homolytic O–O bond cleavage generates an OH species and one-electron reduced Cpd I, and subsequent proton transfer to this OH species with concomitant electron transfer from the heme yields Cpd I and water. The rate-limiting step at the QM/MM level is O–O cleavage with a barrier of about 13–14 kcal/mol in both the Asp251 and Glu366 channels.

Here, we extend this previous QM/MM work to address the effect of Thr252 mutations on the formation of Cpd I and on the competition between coupling and uncoupling reactions, that is, conversion of Cpd 0 to Cpd I and water as opposed to the ferric resting state and hydrogen peroxide. We cover the wild-type P450cam enzyme and its mutants T252S, T252V, T252A, and T252G. We also consider the effect of an extra water molecule in the active site by means of classical MD simulations and QM/MM calculations for different mutants.

II. Computational Details

Starting from a crystallographic structure (pdb file: 1DZ8), we generated a Cpd 0 model for the T252S, T252V, T252A, and T252G mutants by manually replacing the threonine residue in the wild-type enzyme with serine, valine, alanine, and glycine, respectively. Solvation and protonation procedures followed standard protocols used previously in our group.^{34–36} Asp251 was protonated since it serves as proton source in the present study. The resulting model with a net charge of $-8e$ was neutralized by protonating selected ionic residues at the surface of the enzyme without affecting salt bridges or hydrogen bonds.

The system was solvated using 5891 TIP3P water molecules³⁷ (yielding a total of ca. 25 000 atoms). It was relaxed by energy minimizations and classical molecular dynamics (MD) simulations using the CHARMM22 force field³⁸ as implemented in the CHARMM³⁹ program. Throughout all MD simulations, the coor-

dinates of the entire heme unit and the coordinating Cys357 as well as the outer 8 Å of the solvent layer were kept fixed.

The applied QM/MM methodology is analogous to that used in our group in related studies.^{33–36} Therefore, only some aspects relevant to the present work are presented here. An electronic embedding scheme⁴⁰ was adopted in the QM/MM calculations; that is, the MM charges were included in the one-electron Hamiltonian of the QM part, and the QM/MM electrostatic interactions were evaluated from the QM electrostatic potential and MM partial charges. No cutoffs were introduced for the nonbonding MM and QM/MM interactions. Hydrogen link atoms and the charge shift model⁴¹ were employed to treat the QM/MM boundary. The TURBOMOLE⁴² program was used for the QM calculations, while the CHARMM22 force field was run through the DL_POLY⁴³ code for the treatment of the MM part. The QM/MM calculations were performed with the ChemShell package⁴⁴ that integrates the TURBOMOLE and DL_POLY programs, and geometry optimizations were carried out using the HDLC optimizer⁴⁵ implemented in ChemShell.

The QM part was treated by the UB3LYP⁴⁶ density functional method with a LACVP⁴⁷ small-core ECP basis set (B1), that is, double ζ on Fe and 6-31G⁴⁸ on the rest of the atoms. The MM part was described by the CHARMM22 force field. For improved accuracy, all calculations were repeated using the larger TZVP^{49,50} basis set (B2) on all atoms.

The optimized active region was defined to include all residues and water molecules within 6 Å of any atom of the core region. This results in ca. 1400 atoms to be optimized, which belong to the iron–dioxygen–porphyrin complex, camphor, and the amino acid residues and water molecules around the active site. All minima and transition states (TS) reported in this paper were fully optimized.

QM Region: For our present QM/MM calculations, we employed QM regions analogous to those adopted for the wild-type enzyme in our previous work³³ (see Figure 1). For the wild-type enzyme (model A): iron–porphine (without heme side chains), sulfur atom of Cys357, distal O₂H moiety, the C ^{β} H–O ^{α} H unit of Thr252, Wat901, and the C ^{β} H₂–C ^{α} (=O ^{δ} 1)(–O ^{δ} 2H) unit of Asp251 (Figure 1). For the serine mutant (model B), the threonine side chain was replaced by the serine side chain, and hence only the C ^{α} H₃–O ^{α} H unit was included in the QM region. The QM regions for the valine, alanine, and glycine mutants were obtained analogously (see models C, E, and G in Figure 1), with the C ^{α} H₃–C ^{β} H–C ^{α} H₃ unit (C) and the C ^{α} H₄ unit (E) being part of the QM region. Finally, an extra water molecule (WatS) in the QM region extends models C, E, and G to models D, F, and H, respectively.

III. Results and Discussion

1. Classical MD Results. Classical MD simulations were performed to check whether the Asp251 channel can support an additional water molecule (WatS) to form a more extended hydrogen-bonding network. The native enzyme has been studied

- (28) Shaik, S.; Kumar, D.; de Visser, S. P.; Altun, A.; Thiel, W. *Chem. Rev.* **2005**, *105*, 2279–2328.
 (29) Ogliaro, F.; De Visser, S. P.; Cohen, S.; Sharma, P. K.; Shaik, S. *J. Am. Chem. Soc.* **2002**, *124*, 2806–2817.
 (30) Kumar, D.; Hirao, H.; De Visser, S. P.; Zheng, J.; Wang, D.; Thiel, W.; Shaik, S. *J. Phys. Chem. B* **2005**, *109*, 19946–19951.
 (31) Kamachi, T.; Shiota, Y.; Ohta, T.; Yoshizawa, K. *Bull. Chem. Soc. Jpn.* **2003**, *76*, 721–732.
 (32) Harris, D. L.; Loew, G. H. *J. Am. Chem. Soc.* **1998**, *120*, 8941–8948.
 (33) Zheng, J.; Wang, D.; Thiel, W.; Shaik, S. *J. Am. Chem. Soc.* **2006**, *128*, 13204–13215.
 (34) Schöneboom, J. C.; Thiel, W. *J. Phys. Chem. B* **2004**, *108*, 7468–7478.
 (35) Schöneboom, J. C.; Lin, H.; Reuter, N.; Thiel, W.; Cohen, S.; Ogliaro, F.; Shaik, S. *J. Am. Chem. Soc.* **2002**, *124*, 8142–8151.
 (36) Altun, A.; Thiel, W. *J. Phys. Chem. B* **2005**, *109*, 1268–1280.
 (37) Jorgensen, W. L.; Chandrasekhar, J.; Madura, J. D.; Impey, R. W.; Klein, M. L. *J. Chem. Phys.* **1983**, *79*, 926–935.
 (38) MacKerell, A. D., Jr.; et al. *J. Phys. Chem. B* **1998**, *102*, 3586–3616.
 (39) Brooks, B. R.; Brucoleri, R. E.; Olafson, B. D.; States, D. J.; Swaminathan, S.; Karplus, M. *J. Comput. Chem.* **1983**, *4*, 187–217.

- (40) Bakowies, D.; Thiel, W. *J. Phys. Chem.* **1996**, *100*, 10580–10594.
 (41) Sherwood, P.; De Vries, A. H.; Collins, S. J.; Greatbanks, S. P.; Burton, N. A.; Vincent, M. A.; Hillier, I. H. *Faraday Discuss.* **1997**, *106*, 79–92.
 (42) Ahlrichs, R.; Bär, M.; Häser, M.; Horn, H.; Kölmel, C. *Chem. Phys. Lett.* **1989**, *162*, 165–169.
 (43) Smith, W.; Forester, T. R. *J. Mol. Graph.* **1996**, *14*, 136–141.
 (44) Sherwood, P.; et al. *J. Mol. Struct.* **2003**, *632*, 1–28.
 (45) Billeter, S. R.; Turner, A. J.; Thiel, W. *Phys. Chem. Chem. Phys.* **2000**, *2*, 2177–2186.
 (46) Becke, A. D. *J. Chem. Phys.* **1993**, *98*, 5648–5652.
 (47) Hay, P. J.; Wadt, W. R. *J. Chem. Phys.* **1985**, *82*, 299–310.
 (48) Hehre, W. J.; Ditchfield, K.; Pople, J. A. *J. Chem. Phys.* **1972**, *56*, 2257–2261.
 (49) Schäfer, A.; Huber, C.; Ahlrichs, R. *J. Chem. Phys.* **1994**, *100*, 5829–5835.
 (50) Schäfer, A.; Horn, H.; Ahlrichs, R. *J. Chem. Phys.* **1992**, *97*, 2571–2577.

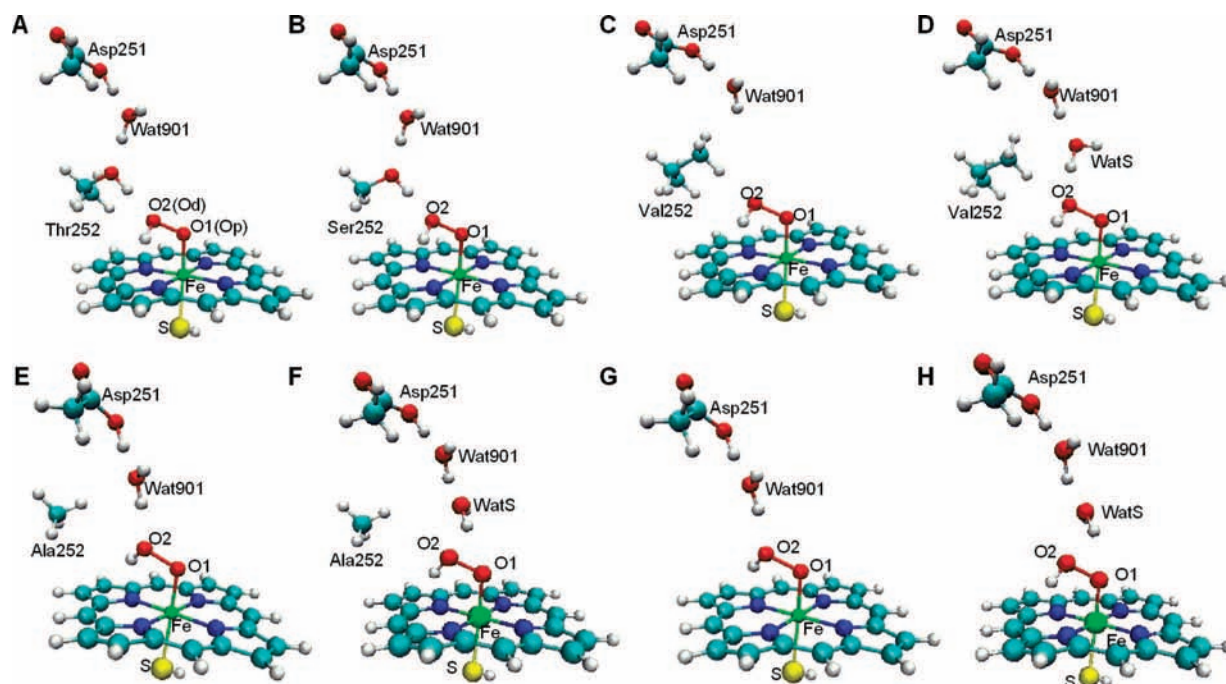


Figure 1. QM regions for the wild-type enzyme and its mutants. Models A, B, C, E, and G represent the native enzyme of P450cam, the T252S mutant, the T252V mutant, the T252A mutant, and the T252G mutant, respectively. Models D, F, and H extend models C, E, and G, respectively, with an extra water molecule (WatS).

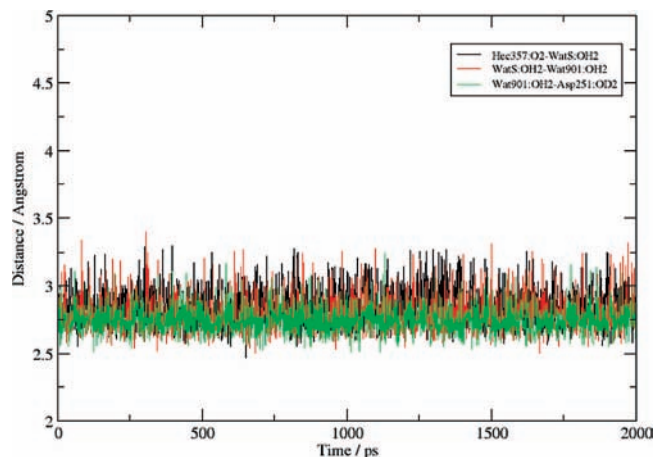


Figure 2. Monitoring the mobility of the extra water molecule (WatS) in the T252A mutant (for atom labels, see Figure 1F; Hec is the porphine-FeO₂ unit).

previously in this regard, and it was found that the extra water molecule leaves the active site.⁵¹ In the present MD simulations on the serine, valine, alanine, and glycine mutants of Cpd 0, we checked the mobility of WatS and, at the same time, tested the stability of the hydrogen-bonding network between Asp251 and the FeO₂H moiety.

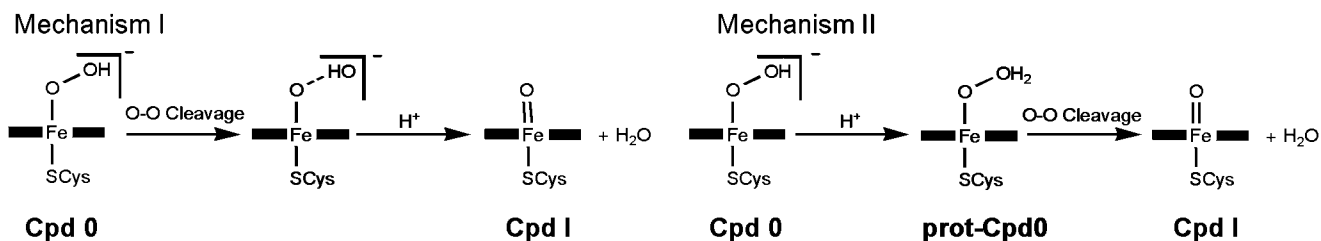
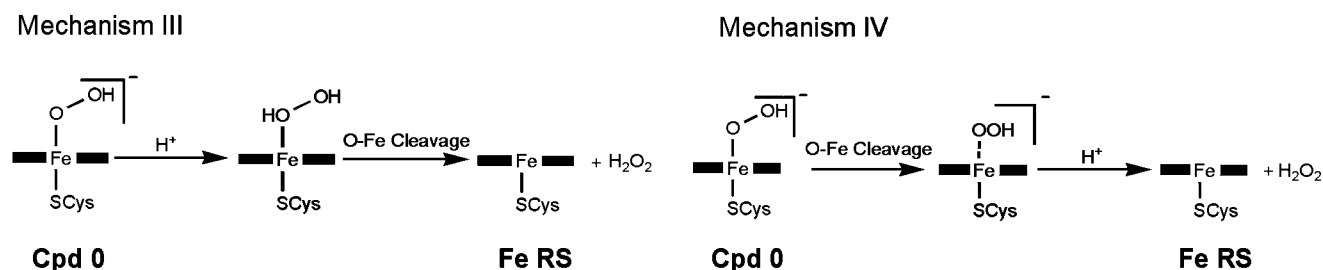
Substitution of threonine by alanine generates some empty space in the distal pocket so that WatS can find a stable position between Wat901 and the FeO₂H moiety. The classical MD results for the alanine mutant in Figure 2 show that Wat901 and WatS do not escape from the protein pocket during the 2 ns simulation. WatS stays close to the FeO₂H moiety for most of the time, whereas Wat901 forms two hydrogen bonds with

WatS and the Asp251 residue (confirmed by average distances of 2.80 ± 0.13 and 2.75 ± 0.10 Å for WatS:OH₂-Wat901:OH₂ and Wat901:OH₂-Asp251:OD₂, respectively). The distance between the O₂H moiety and the oxygen atom of WatS also remains around 3 Å (2.85 ± 0.13 Å). Hence all these hydrogen bonds are conserved in the alanine mutant. This is consistent with the crystal structure of the T252A mutant which shows an extra water molecule (not present in the wild-type enzyme) near the O₂ (distal oxygen) binding site of the mutant.^{11,21} Likewise, the 2 ns MD simulations for the valine and glycine mutants confirm the stability of the additional water molecule (see Figures S2 and S3 in the Supporting Information). By contrast, the extra water molecule is not stable in the serine mutant since it escapes from the distal pocket very early in the MD simulation (see Figure S1 in the Supporting Information), in analogy to the behavior of the wild-type enzyme.

2. Survey of Possible Reaction Mechanisms. Scheme 2 shows the four mechanisms that were considered in the QM/MM calculations. In each case, the crystallographic water molecule W901 (in combination with WatS in models D, F, and H) supports proton transfer from Asp251 to the X252 residue (X = threonine, serine, valine, alanine, and glycine). The proton transferred to the FeO₂H moiety comes from the hydroxy group of threonine in the WT enzyme or serine in the T252S mutant. In the absence of a hydroxy group, such as in the valine, alanine, and glycine mutants, it is transferred from the closest water molecule, which is Wat901 in models C, E, and G, and WatS in models D, F, and H. The proton-donating sites are replenished by proton transfer along the hydrogen-bonding network in the Asp251 channel. The following mechanisms were studied for coupling (I,II) and uncoupling (III,IV).

Mechanism I: Initially, the O–O bond is cleaved homolytically to generate an OH species and a one-electron reduced Cpd

(51) Zheng, J.; Altun, A.; Thiel, W. *J. Comput. Chem.* **2007**, *28*, 2147–2158.

Scheme 2. Mechanisms for (a) Cpd I Formation (Coupling Reaction) and (b) Ferric Resting State Formation (Uncoupling Reaction)**(a) Coupling reaction****(b) Uncoupling reaction**

I. A subsequent proton transfer to the OH species with a concomitant electron transfer from the heme yields Cpd I and water.³³

Mechanism II: A proton is transferred to the distal oxygen atoms of the hydroperoxo group to form protonated Cpd 0 (prot-Cpd 0: FeOOH_2), followed by heterolytic O–O bond cleavage that generates Cpd I and water.³³ In the Asp251 channel, we were unable to locate a stable prot-Cpd 0 minimum for any of the mutants, as in the case of the native enzyme.³³ We thus conclude that mechanism I is preferred and only discuss this mechanism for the coupling reaction.

Mechanism III: A proton is transferred to the proximal oxygen atom of the hydroperoxo group to form FeH_2O_2 , accompanied by heterolytic O–Fe bond cleavage that generates the ferric resting state and hydrogen peroxide.

Mechanism IV: Initially, the O–Fe bond is cleaved homolytically to generate an OOH radical, followed by a proton transfer to the OOH group to yield the ferric resting state and hydrogen peroxide. Mechanism IV is calculated to be much less favorable than mechanism III for the uncoupling reaction since the O–Fe cleavage reaction always requires much activation. Inclusion of an extra water molecule in the T252V, T252A, and T252G mutants has only a minor effect on this barrier which remains high. Therefore, we do not discuss the corresponding results here but only document them in the Supporting Information.

3. QM/MM Results. The QM/MM optimized structures for the QM region of Cpd 0 are shown in Figure 1 for the native enzyme and its mutants. In the native enzyme, Cpd 0 has a doublet ground state which is more stable than the quartet state both in the gas phase^{29,31} and the enzyme environment.³³ The same also holds for the T252X mutants, and we shall therefore only discuss the doublet state in this paper. We have carried out full QM/MM optimizations for all relevant doublet species using both the B1 and B2 basis set. The geometries and energies

obtained with the two basis sets are generally similar. Optimized geometries are shown in Figures 3 and 4 and in Figures S4–S16 of Supporting Information. Table 1 lists the relative energies of all optimized stationary points (both B1 and B2 values, relative to Cpd 0). In the text, we shall quote energy values computed with the larger B2 basis set (unless noted otherwise).

In addition, we have also performed full QM/MM optimizations for the lowest quartet and sextet states of Cpd 0 in the wild-type enzyme and each mutant using the B1 basis set. The Supporting Information documents the corresponding results along with those for the doublet ground state in detail, providing QM, MM, and QM/MM energies, spin densities, group charges, and selected geometric parameters (Tables S2–S13). The Supporting Information also contains spin densities and group charges for the doublet states of the optimized stationary points of mechanisms I, III, and IV (B1 basis).

3.1. Wild-Type Enzyme. Coupling Reaction: We have previously investigated the conversion of Cpd 0 to Cpd I in the wild-type enzyme at the QM/MM level using the B1 basis.³³ We have now reoptimized the stationary points using the B2 basis, which leads to minor changes only. The transition states for the initial O–O cleavage and the subsequent proton transfer lie 14.3 and 11.7 kcal/mol above Cpd 0, respectively, and the overall reaction energy is calculated to be -3.7 kcal/mol.

Uncoupling Reaction: In the favored mechanism III, the proton is transferred through the Asp251–Wat901–Thr252–HOOFe hydrogen-bonding chain to O1 (proximal oxygen) which triggers O–Fe bond cleavage and generates the ferric resting state and hydrogen peroxide. Figure 3 shows the corresponding QM/MM optimized structures. According to the QM/MM calculations, the reaction proceeds in a single step, with an activation barrier of 27.0 kcal/mol, and is endothermic by 6.4 kcal/mol. The formed hydrogen peroxide has almost zero spin density (see Supporting Information) in the product (ferric resting state, FeRS). The Fe–O1 distance increases from 1.87 Å in Cpd 0 to

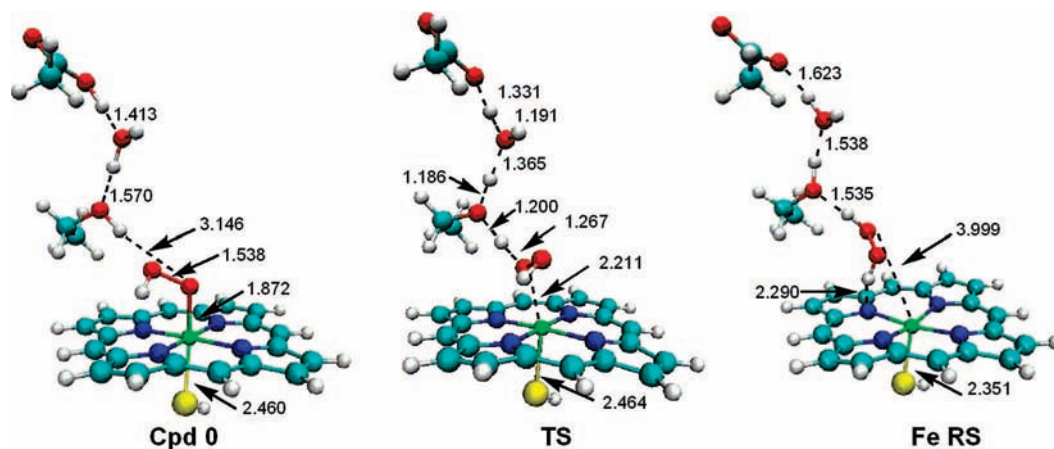


Figure 3. Optimized geometries (UB3LYP/B1/CHARMM) for the uncoupling reaction in the wild-type enzyme. Only the QM region is shown.

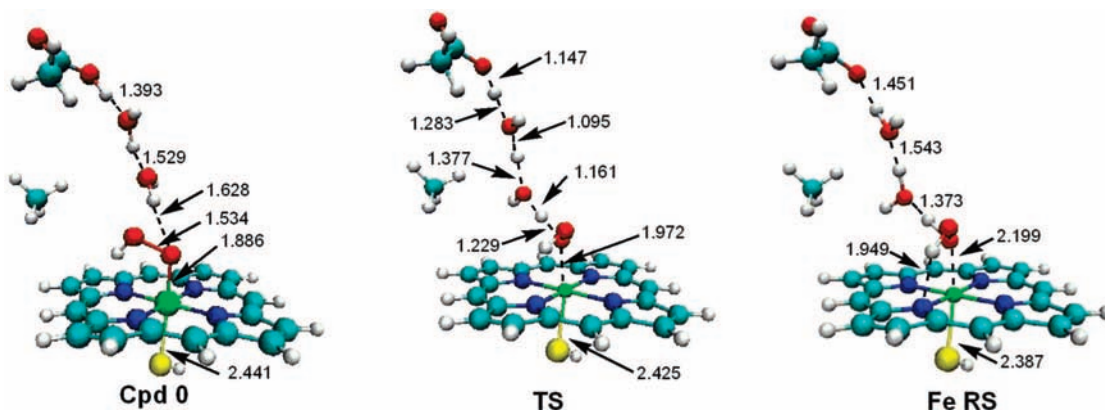


Figure 4. Optimized geometries (UB3LYP/B1/CHARMM) for the uncoupling reaction in the T252A mutant in the presence of an extra water molecule (WatS). Only the QM region is shown.

Table 1. Computed Relative Energies (kcal/mol) for Optimized Stationary Points Using Basis Sets B1/B2 (with respect to Cpd 0)^a

mechanism	species	model A WT	model B T252S	model C T252V	model D T252V+W	model E T252A	model F T252A+W	model G T252G	model H T252G+W
I	TS1	14.4/14.3	15.8/15.6	17.1/17.1	19.0/18.9	17.4/17.1	17.5/17.3	18.8/17.9	19.3/18.9
	IC1	11.7/10.9	9.4/8.4	11.4/11.0	16.0/15.4	9.5/7.7	15.2/16.0	5.7/5.9	11.5/11.5
	TS2	14.3/11.7	11.4/11.6	14.6/15.0	18.1/18.1	12.3/10.6	16.7/17.0	7.1/7.8	11.7/11.9
	Cpd I	-0.2/-3.7	-0.4/-3.8	-0.2/-2.6	7.1/-0.6	-2.0/-2.3	2.5/-3.0	-2.6/-3.4	2.0/-5.0
III	TS	26.6/27.0	22.3/23.1	24.5/26.5	19.4/19.5	27.6/29.1	11.7/11.9	28.8/28.2	11.4/12.0
	Fe RS	7.2/6.4	11.8/8.0	7.5/6.4	13.4/7.2	5.6/-0.1	4.3/2.4	4.4/-1.0	4.8/1.7

^a For notation see text; for models A–H, see Figure 1; +W denotes the presence of an extra water molecule. All energies refer to geometries that are fully optimized using the corresponding basis set (B1/B2).

4.00 Å in FeRS, and the O1–O2 distance is 1.51 Å, as expected for hydrogen peroxide.

In the native P450cam enzyme, the coupling reaction is thus computed to be much more facile than uncoupling, and there should be no release of hydrogen peroxide. This agrees with experiment where 5-exohydroxycamphor is found as the only product.¹⁸

3.2. T252S Mutant. In this mutant, there is only one water molecule (Wat901) in the distal pocket of the enzyme since a manually added water molecule (WatS) quickly leaves the pocket during MD simulation (see above and Figure S1 in Supporting Information). However, like threonine in the wild-type enzyme, serine has a hydroxyl group and can thus form a proton transfer channel from Asp251 to the FeOOH moiety through Wat901 and its hydroxyl group.

Coupling Reaction: Figure S4 in the Supporting Information presents the QM/MM optimized structures for the coupling

reaction of the serine mutant. The barrier for O–O bond cleavage is 15.6 kcal/mol, and the energy of the first intermediate (IC1) is 8.4 kcal/mol. The transition state for the subsequent proton transfer from Asp251 via the water molecule (Wat901) to serine lies at 11.6 kcal/mol. The overall reaction is exothermic by -3.8 kcal/mol. After proton release, the side chain of Asp251 rotates back to form a salt bridge with Arg186 as shown in Figure S4 in Supporting Information. The spin density and charge of the OH group in the first intermediate (IC1) are -0.6 and -0.2, indicating that OH will not behave as a “perfect” radical in IC1 due to the strong hydrogen-bonding interactions with Ser252 and the FeO unit (as in the case of the wild-type enzyme³³). Overall, the coupling reaction is very similar in the T252S mutant and the wild-type enzyme, both electronically and mechanistically. The rate-limiting barrier is slightly higher in the T252S mutant (15.6 vs 14.3 kcal/mol in the wild-type enzyme).

Uncoupling Reaction: The optimized structures are shown in Figure S5 in Supporting Information. Like in the wild-type enzyme, the reaction proceeds in one step, with an energy barrier of 23.1 kcal/mol, and is endothermic by 8.0 kcal/mol. In the transition state and the product, Ser252 and Asp251 have zero spin density, consistent with a proton-assisted heterolytic O–Fe bond cleavage. The O–O distance stays at around 1.5 Å during the reaction, whereas the Fe–O1 distance increases from 1.87 Å in Cpd 0 to 2.24 Å in TS1 and to 3.71 Å in the product, thus reflecting the formation of hydrogen peroxide and the cleavage of the O–Fe bond.

A comparison of the computed rate-limiting barriers for the T252S mutant shows that the coupling reaction is favored over the uncoupling reaction by 7.5 kcal/mol, less so than in the wild-type enzyme where the difference in the computed barriers is 12.8 kcal/mol. Experimentally, the serine mutant retains a high ratio in the coupling of oxygen consumption to *d*-camphor hydroxylation with some H₂O₂ formation being observed (15% of oxygen consumption relates to hydrogen peroxide and 85% to *d*-camphor hydroxylation).^{7,19} The QM/MM calculations thus give the correct qualitative trend that uncoupling becomes more facile in the T252S mutant compared with the wild-type enzyme, but they are not accurate enough to provide quantitative predictions.

3.3. T252V Mutant. As noted before, the T252V mutant has enough space to accommodate an extra water molecule (WatS) in the distal pocket of the enzyme (see above and Figure S2 in Supporting Information). We have therefore studied its reactions without and with WatS (see models C and D in Figure 1). Figures S6–S9 in the Supporting Information show the QM/MM optimized structures (QM region only).

Coupling Reaction without WatS: Similar to the wild-type enzyme and the T252S mutant, the coupling reaction starts with O–O cleavage followed by proton transfer from Asp251 to the formed OH species either directly through Wat901 or through the methyl group of valine. The latter path through the methyl group is unfavorable (transition state at 26 kcal/mol) and will thus not be discussed. On the preferred path through Wat901, the transition states for the two steps lie at 17.1 and 15.0 kcal/mol, respectively, and the intermediate (IC1) is 11.0 kcal/mol above Cpd 0. Judging from the computed spin density (–0.97) IC1 contains an almost “pure” OH radical. After the proton transfer, Asp251 moves back to form a hydrogen bond with Arg186; in this product conformation, Asp251 has zero spin density and a Mulliken group charge of almost –0.5 e.

Coupling Reaction with WatS: The introduction of WatS extends the hydrogen-bonding network in the Asp251 channel. It does not affect the computed energy profile much. The two transition states are raised in energy slightly, to 18.9 and 18.1 kcal/mol, respectively. The intermediate again contains an OH radical (spin density of –0.98), and the formation of Cpd I is again roughly thermoneutral (–0.6 kcal/mol). The presence of an extra water molecule (WatS) in the protein pocket of the T252V mutant thus does not have a significant influence on the coupling reaction.

Uncoupling Reaction without WatS: As in the case of the T252V mutant, only a concerted process is found, with a barrier of 26.5 kcal/mol and an endothermicity of 6.4 kcal/mol. The O–Fe distance increases from 1.86 Å in Cpd 0 to 2.10 Å in the transition state and 4.04 Å in the product. The H₂O₂ moiety has zero spin density and a total charge of –0.1 in the product, consistent with the formation of hydrogen peroxide.

Uncoupling Reaction with WatS: The incorporation of an extra water molecule into the Asp251 channel lowers the computed barrier appreciably, by 7.0 to 19.5 kcal/mol, while the endothermicity changes only slightly to 7.2 kcal/mol. In the product, the spin density and Mulliken charge on H₂O₂ are 0.0 and –0.4 e, respectively.

Comparing the different mechanistic scenarios for the T252V mutant, we find similar barriers for coupling and uncoupling in the presence of WatS (18.9 vs 19.5 kcal/mol) and a slightly lower rate-limiting barrier for coupling in the absence of WatS (17.1 kcal/mol). Considering the limited accuracy of our calculations, we can only conclude qualitatively that these reactions should be competitive and that one should expect both *d*-camphor hydroxylation and H₂O₂ formation in the T252V mutant.

3.4. T252A Mutant. As in the case of the T252V mutant, we have studied the coupling and uncoupling reactions both in the absence and presence of an additional water molecule (WatS). The QM/MM optimized structures are shown in Figure 4 and Figures S10–S12 in the Supporting Information (QM regions only).

Coupling Reaction without WatS: The transition states for the two steps are located at 17.1 and 10.6 kcal/mol above Cpd 0. The rate-limiting barrier for the initial O–O cleavage is 2.8 kcal/mol higher than in the wild-type enzyme. The O–O distance increases from 1.53 Å in Cpd 0 to 2.60 Å in the intermediate (IC1), reflecting cleavage of the O–O bond. The O–Fe distance is 1.66 Å in the product, confirming the formation of Cpd I.

Coupling Reaction with WatS: Inclusion of an extra water molecule (i.e., going from model E to model F in Figure 1) has a negligible effect on the rate-limiting barrier for the initial O–O cleavage (17.3 kcal/mol) but raises the energies of the intermediate and the transition state for proton transfer appreciably. The overall exothermicity is also not affected much (–3.0 kcal/mol). After proton release, the side chain of Asp251 rotates back to form a salt bridge with Arg186 in the product.

Uncoupling Reaction without WatS: The proton transfer and the O–Fe bond cleavage occur in a concerted manner, with an activation barrier of 29.1 kcal/mol, which is about 12 kcal/mol higher than that for the coupling reaction in this mutant.

Uncoupling Reaction with WatS: Upon extension of the hydrogen-bonding network by WatS, the reaction remains concerted, but its barrier is reduced dramatically to 11.9 kcal/mol. The reaction energy does not change much (endothermic by 2.4 kcal/mol).

Comparing the computed barriers for the T252A mutant, we conclude that the uncoupling reaction is favored over the coupling reaction by about 5 kcal/mol, provided that an additional water molecule can enter the Asp251 channel close to the active site. If this is the case, the QM/MM results imply that formation of hydrogen peroxide should be dominant. This is consistent with the available experimental evidence.^{12,21} Since Cpd I is not formed under these conditions, the experimentally observed epoxidation in the T252A mutant must be due to another oxidant, with Cpd 0 being an obvious candidate.¹⁴ DFT calculations for gas-phase model systems indicate that Cpd 0 can indeed act as an oxidant for epoxidation, even though it is far less reactive than Cpd I.¹⁷ It would seem worthwhile to address the possible competition between epoxidation and uncoupling in the T252A mutant in future QM/MM work.

3.5. T252G Mutant. Since the T252G mutant also provides sufficient space for an extra water molecule (WatS) close to

the active site, we studied the coupling and uncoupling reactions again in the absence and in the presence of WatS. Figures S13–S16 in the Supporting Information show the optimized QM/MM structures (QM regions only). Glycine is part of the MM region since it has no side chain that could be included in the QM region.

Coupling Reaction without WatS: The rate-limiting barrier for the initial O–O cleavage is 17.9 kcal/mol, that is, of similar magnitude as in the T252V and T252A mutants, but higher than in the wild-type enzyme. The intermediate (IC1) and the transition state for proton transfer from Asp251 to the OH radical lie 5.9 and 7.8 kcal/mol above Cpd 0, respectively. The overall reaction is exothermic by -3.4 kcal/mol.

Coupling Reaction with WatS: As in the other mutants, the presence of WatS molecule does not have much effect on the coupling reaction. Its inclusion raises the barrier for the initial O–O cleavage slightly to 18.9 kcal/mol and also increases the relative energies of the intermediate (11.5 kcal/mol) and the second transition (11.9 kcal/mol). The reaction remains exothermic (-5.0 kcal/mol).

Uncoupling Reaction without WatS: As in the case of the T252A mutant, the proton transfer from Asp251 via Wat901 to O1 and the cleavage of the Fe–O1 bond occur in a concerted reaction. The activation energy for the formation of H₂O₂ is 28.2 kcal/mol and thus about as high as that of the T252A mutant.

Uncoupling Reaction with WatS: The inclusion of WatS allows the formation of a more extended hydrogen-bonding network that provides a much better path for proton transfer between the proton source (Asp251) and the proton acceptor (O1). The barrier is thus reduced drastically to 12.0 kcal/mol, without affecting the reaction energy much (endothermic by 1.7 kcal/mol).

At first sight, it seems surprising that the uncoupling reaction with WatS has a significantly lower barrier in the T252A and T252G mutants than in the T252V mutant. Closer inspection of the QM/MM optimized structures of Cpd 0 offers an explanation: In the alanine and glycine mutants, WatS is hydrogen-bonded to both oxygen atoms of the FeO₂ unit with distances of 1.5 to 1.7 Å. In the T252V mutant, however, the steric demands of the valine residue change the hydrogen-bonding network such that WatS is hydrogen-bonded to the distal oxygen only so that the proton transfer to the proximal oxygen is hindered and requires more activation. As a consequence, a clear preference for uncoupling results only for the T252A and T252G mutants.

IV. Summary and Conclusions

Four mutants (Thr252Ala, Thr252Val, Thr252Gly, Thr252Ser) of P450cam have been targeted to investigate mutation effects on the formation of Cpd I. We have studied two competing reactions at the QM/MM level, which both originate from Cpd 0 and require proton transfer toward Cpd 0: the conversion of Cpd 0 to Cpd I and water (coupling reaction), and the regeneration of the ferric resting state with concomitant formation of hydrogen peroxide (uncoupling reaction). For each reaction, we have considered two mechanisms: either first bond cleavage in the FeOOH moiety followed by proton transfer in the Asp251 channel, or both steps in reverse order. Only the more facile of these two pathways has been discussed in the text for each reaction (mechanisms I and III), while the other results are only presented as Supporting Information.

The stability of an additional water molecule in the distal pocket has been tested for all four mutants by classical MD simulations. This extra water molecule quickly escapes from the distal pocket of the T252S mutant (as in the case of the native enzyme) but remains stable during 2 ns simulations of the T252A, T252G, and T252V mutants. Hence, for these three mutants, the reactions have been studied both without and with an additional water molecule.

In the coupling reaction, the initial and rate-limiting step is a homolytic O–O bond cleavage followed by a concomitant proton and electron transfer that yields Cpd I and water. In the wild-type enzyme, the O–O bond cleavage has a barrier of 14 kcal/mol that increases slightly to 16 kcal/mol in the T252S mutant and 17–18 kcal/mol in the T252A, T252V, and T252G mutants. The presence of the extra water molecule (WatS) in the T252A, T252V, and T252G mutants has only marginal effects on this barrier. The transition state for the initial O–O cleavage is rate-limiting in all five enzymes considered. Since the mutations as well as the additional water molecule mainly affect the subsequent proton transfer, it is reasonable that neither of these modifications causes any significant effect on the rate-limiting step of the coupling reaction.

The uncoupling reaction involves a proton transfer from Asp251 via a hydrogen-bonding network to the distal oxygen atom (O1) accompanied by O–Fe bond cleavage that leads to the ferric resting state and hydrogen peroxide. An alternative two-step mechanism with initial O–Fe bond cleavage is less favorable. Without the extra water molecule, the energy barrier of the concerted mechanism is 25–28 kcal/mol in the wild-type enzyme and the valine, alanine, and glycine mutants. The presence of an extra water molecule (WatS) drastically reduces this barrier to 11 kcal/mol for the T252A and T252G mutants and to 19 kcal/mol for the T252V mutant.

According to the experimental data, the coupling reaction is more favorable in the wild-type enzyme and the serine mutant, with 100 and 85% coupling (formation of Cpd I), respectively. In the serine mutant, uncoupling (formation of hydrogen peroxide) accounts for 15% of the O₂ consumption. The uncoupling reaction dominates in the T252A and T252G mutants, where only 3–5% of the O₂ is consumed to form Cpd I. In the T252V mutant, both reactions occur with similar probability.

If the effect of an additional water molecule is not taken into account, the present QM/MM calculations would disagree with experimental results; that is, all mutants would behave like the wild-type enzyme and prefer coupling over uncoupling. An additional water molecule in the Asp251 channel has only a minor influence on the formation of Cpd I. However, consistent with experimental observations that direct contact between solvent water and the heme active site is responsible for uncoupling, an extra water molecule has a significant effect on the uncoupling reaction. In case of the T252A and T252G mutants, the barrier of the uncoupling reaction is reduced dramatically such that the coupling reaction becomes disfavored, in line with experiment. For the T252V mutant, both reactions are observed experimentally, which can again only be rationalized if an additional water molecule is taken into account. The competition between the coupling and uncoupling reactions and the effects of the extra water molecule are illustrated by the energy profiles for the wild-type enzyme (Figure 5) and the T252A mutant (Figure 6). It is conceivable that there are other P450 systems (e.g., with other substrates and/or other mutations) where a single additional water molecule may also play a

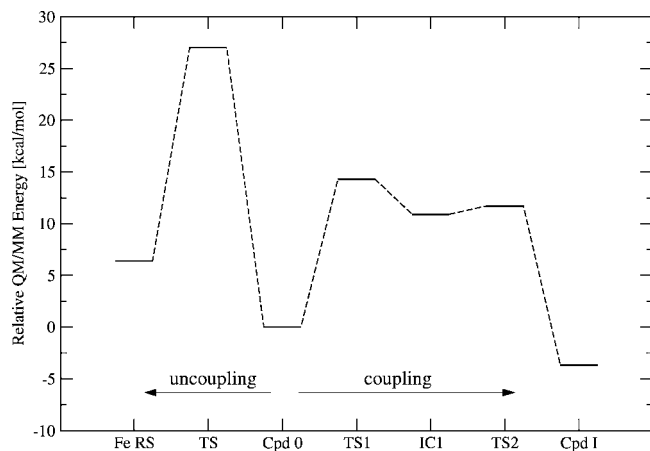


Figure 5. Energy profile (UB3LYP/B2/CHARMM) of the coupling and uncoupling reaction in the wild-type enzyme.

decisive mechanistic role, and it is therefore generally advisable in theoretical work to check this possibility by explicit simulation.

The present QM/MM results agree with the available experimental evidence and thus offer an atomistic explanation for the role of the Thr252 residue in the reactions of Cpd 0. Thr252 is a highly specific proton donor to the distal oxygen atom of Cpd 0, and the preference for the coupling reaction in the wild-type enzyme is based on this specificity. If Thr252 is replaced by small aliphatic residues, an additional water molecule can enter the active site and establish proton transfer channels to both oxygen atoms of the FeOOH moiety. Optimum hydrogen-bonding networks can be formed in the T252A and T252G mutants, which lower the barriers to proton transfer substantially and lead to a preference for uncoupling. This effect is less pronounced in the T252V mutant with the sterically more demanding valine residue, and hence both reactions can occur in this case. Replacing Thr252 with a structurally similar serine residue causes only relatively minor changes since the required proton transfer can make use of the OH group that is present in

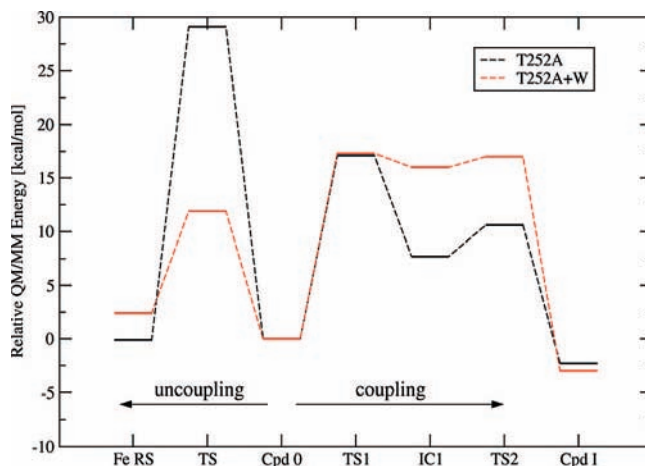


Figure 6. Energy profiles (UB3LYP/B2/CHARMM) of the coupling and uncoupling reaction with and without an extra water in the T252A mutant.

both residues, without the need to involve an extra water molecule. The difference between the computed rate-limiting barriers for coupling and uncoupling is smaller in the T252S mutant than in the wild-type enzyme, which is qualitatively consistent with the slight decrease in the observed specificity.

Acknowledgment. This work was supported by the Max Planck Society.

Supporting Information Available: MD results for the T252S, T252V, and T252G mutants. Energies, spin densities, and group charges for mechanisms I, III, and IV. Geometric parameters for mechanisms I and III. Optimized geometries of the stationary points of mechanisms I, III, and IV. Complete references 38 and 44. This material is available free of charge via the Internet at <http://pubs.acs.org>.

JA808744K